IJHSR
ijhighschoolresearch.org
RESEARCH ARTICLE

Multiplexed Immunohistochemistry Reveals Cancer-Reactive Germinal Centers are Enriched with $CD8^+$ and T_{fh} Cells

Aadi Bhattacharya

Rye Country Day School, 3 Cedar Street, Rye, NY, 10580, USA; aadi.gbh@gmail.com
Mentors: Dr. Ramin Herati, Ms. Jen Doran

ABSTRACT: Lung cancer kills hundreds of thousands of people worldwide each year. Sites of immune cell activity called germinal centers (GCs) in lymph nodes are associated with improved survival outcomes in cancer patients. The mechanisms by which GCs influence patient survival are not well-understood but could hold the key to further improving survival. Our goal was to investigate the differences in the physical and cellular characteristics of healthy and cancer-reactive GCs to help elucidate the role of GCs in patients' response to cancer. To do so, GCs in a lung cancer-draining mediastinal lymph node were compared to GCs in a non-cancerous tonsil. We used multiplexed immunohistochemistry for 22 antibody targets to analyze the samples, thereby allowing simultaneous analysis of multiple biomarkers in a tissue sample. Although most cell types were present in similar proportions in the GCs of each tissue, there were more $CD8^+$ T cells and follicular helper $CD4^+$ T cells in the GCs of the cancer-draining node. A better understanding of the role of these cell types may lead to improved outcomes for lung cancer patients.
KEYWORDS: Biomedical and Health Sciences; Immunology; Cancer; Germinal Centers.

Introduction

Of all cancers, lung cancer is the leading cause of death in the world, killing more than 160,000 people each year in the US alone.[1] Research into the causes and treatments of lung cancer shows that the immune system plays a vital role against the disease.[2] In particular, tertiary lymphoid structures containing germinal centers (GCs) have been linked with improved survival outcomes in cancer patients.[3] GCs are typically found in secondary lymphoid organs (SLOs), such as lymph nodes and tonsils.[4] Still, their role in cancer is not well-understood. The cellular composition of tumor draining lymph nodes is also not widely studied, and little is known about the levels of specific T cell and B cell subgroups in comparison to healthy SLOs.[5]

Although the presence of GCs is associated with improved survival likelihood,[3-7] it is unknown which specific aspects of immunobiology are the most relevant. There are known relationships between T follicular helper (Tfh) $CD4^+$ cells, B cells, and $CD8^+$ T cells that are associated with increased survival in cancer patients.[8-14] It has been hypothesized that interactions of these adaptive immune cells in the GCs may contribute to this result. However, little is known about whether cancer-reactive and non-cancer-reactive GCs differ in biology, although a previous study comparing healthy tonsil and healthy lymph node GCs found few cellular differences between the two.[15] Understanding the potential differences between these GCs could help clarify why some patients with cancer-associated GCs have higher survival chances than those without.

Tissue imaging methods that can detect several antibody targets in a sample can be used to study GCs. Conventional means of studying tissues, such as traditional immunofluorescence (IF), single-cell RNA sequencing (scRNA-seq), and flow cytometry, have yielded significant insights into biology but also have drawbacks. Traditional four-parameter IF can retain the spatial data of the tissue but can only resolve a small number of proteins in a tissue sample.[16] In contrast, flow cytometry and scRNA-seq can resolve many more proteins but lose spatial information by dissociating tissue into single-cell suspensions.[16-18] The CO-Detection by IndEXing (CODEX) platform[19,20] aims to overcome these limitations by using reporters with oligonucleotides complementary to oligonucleotide-conjugated antibodies bound to the tissue. Reporters are imaged in groups followed by the removal of reporters and the addition of the next cycle's reporters. This process is repeated cyclically until all antibody targets are resolved. This approach gathers detailed cellular and biomolecular information in the context of spatial tissue organization and has opened the possibility of studying tissue, including GCs, in unprecedented detail.

We used the CODEX platform to compare cancer-reactive GCs from one thoracic lymph node of a non-small cell lung cancer patient to normal GCs in a tonsil from a different, cancer-free patient. We identified the major T and B cell subsets using high-dimensional clustering.

Methods

One non-small cell lung cancer mediastinal lymph node and one unmatched tonsil were formalin-fixed and paraffin-embedded (FFPE) prior to use in our study. Lymph node and tonsil were provided de-identified by the NYU Center for Biospecimen Research and Development, respectively, after being obtained under informed consent. Clinical information about the patients was not available.

The 5-micron thick tissue was mounted onto a poly-L-lysine-coated coverslip. Tissue staining was performed using the manufacturer's (Akoya Biosciences) instructions. The paraffin was melted at 64°C for twenty minutes, and the sample was incubated in 100% ethanol, then 90% ethanol, 70%

DOI: 10.36838/v5i4.1

ethanol, 50% ethanol, and finally 30% ethanol solutions for five minutes each. The tissue sample was washed in distilled water twice for five minutes each time at room temperature, and subsequently immersed in a 1M solution of sodium citrate (pH=6) at 11 psi for twenty minutes. The beaker was equilibrated to room temperature for ten minutes, after which the staining rack was immersed in distilled water to remove the citrate from the tissue. The tissue was placed into CODEX hydration buffer for four minutes and CODEX staining buffer for five minutes. A blocking buffer solution was also prepared following the manufacturer's instructions. To create the antibody cocktail, 148.7 µL of this blocking solution was added to the dilutions of each of the 22 antibodies studied in this experiment, shown in Table 1, which were selected to identify specific subsets of B, T, epithelial, and cancer cells.[23] Some antibodies used were conjugated by Akoya, while most were manually conjugated. The conjugation process used blank cycles without reporters as controls to verify its success. Every antibody used in this experiment had been validated. CD19, CD20, and CD21 were used to identify B cells, while CD3e and CD45RO were used to identify T cells. CD4 and CD8 expression isolated the $CD4^+$ and $CD8^+$ T cell subgroups, and PD-1 and CD4 were used to isolate T_{fh} cells.

Table 1: List of antibody targets with the concentration and clone of each antibody.

Target	Clone	Dilution	Manufacturer	Conjugation	Target	Clone	Dilution	Manufacturer	Conjugation
PD-1	EPR4877 (2)	1:50	Abcam	Manual	Ki67	B56	1:800	BD Biosciences	Manual
CD45RO	UCHL1	1:100	Akoya	Akoya	CD20	L26	1:100	Akoya	Akoya
PAX5	1H9	1:30	Abcam	Manual	CD21	EP3093	1:2000	Akoya	Akoya
ICOS	D1K2T	1:50	Cell Signaling	Manual	Foxp3	236A/E7	1:50	eBioscience	Manual
Pan-cytokeratin	AE-1/AE-3	1:500	Akoya	Akoya	CD38	EPR4106	1:100	Abcam	Manual
CD8	C8/144B	1:800	Akoya	Akoya	CXCR3	G025H7	1:200	BioLegend	Manual
PD-L1	E1L3N	1:50	Cell Signaling	Manual	T-bet	D6N8B	1:50	Cell Signaling	Manual
Mac/ 2Galectin3	M3/38	1:400	BD Biosciences	Manual	CD19	LE-CD19	1:50	Bio Rad Antibodies	Manual
CD3e	EP449E	1:50	Akoya	Akoya	CD4	EPR6855	1:50	Akoya	Akoya
HLA-DR	EPR3692	1:400	Akoya	Akoya	CD11c	118/A5	1:100	Akoya	Akoya
Vimentin	RV202	1:200	BD Biosciences	Manual	IRF4	1RF4:3E4	1:100	BioLegend	Manual

An empty pipette-tip box was filled to 20% capacity with distilled water to create a humidified chamber. The antibody cocktail was incubated on the tissue sample for three hours. After the staining, the tissue was incubated in CODEX staining buffer for four minutes and then placed in a 1.8% paraformaldehyde (PFA) solution at room temperature for ten minutes. After incubating in the PFA solution, the tissue was washed with PBS. The tissue section was then incubated in ice-cold methanol for ten minutes and washed in PBS. To make the final fixative solution, 20 µL of the CODEX fixative reagent was added to 1 mL of PBS. This solution was added to the tissue in a humidified chamber for twenty minutes.

A photobleaching solution was prepared by adding 25 mL of PBS, 4.5 mL of a 30% H_2O_2 solution, and 0.8 mL of a 1M NaOH solution. The tissue sample was placed in 4 ml of this solution in a six-well plate, sandwiched in between two bright LED panels at 25000 Lux for 45 minutes at room temperature. The tissue was then placed in a fresh 4 mL of the photobleaching solution and repeated. After the photobleaching was finished, the tissue was washed in PBS and refrigerated at 4°C until imaging.

The reporter plate was prepared by adding 2684 µL of nuclease-free water to 330 µL of a 10M CODEX buffer solution, 275 µL of an assay reagent, and 11 µL of a nuclear stain to create the reporter stock solution. For each cycle, every reporter that corresponded to each antibody in that cycle was added to the reporter stock solution at a 1:50 dilution into the corresponding wells of the reporter plate. After the reporter plate was prepared, a 1:2000 DAPI dilution was prepared, and the coverslip was placed into the stage insert. 700 µL of the diluted nuclear stain was added to the tissue sample to identify regions of interest for subsequent imaging.

The CODEX processor (version 1.8, Akoya Biosciences) was used with default parameters, employed background subtraction to remove autofluorescence, deconvolution to reduce out-of-focus light, extended depth of field to enable the collapse of a z-stack into the single best-focus image, and shading correction to adjust for optical shading. Cells were segmented using the default values of the radius, maximum cutoff, minimum cutoff, and size cutoff factor for the region-growing algorithm.[24] The processor, upon completion, produced an FCS file containing the expression levels of each marker for every cell, which was viewed in the CODEX Multiplex Analysis Viewer (MAV) (version 1.5.0.8) to assess the quality of the data.

Results and Discussion

1. Data Quality Assessments:

The data quality was measured qualitatively using both single-antibody expression and multiplexed images generated by MAV. Representative images of the expression for thirteen antibodies are shown (Figure 1).

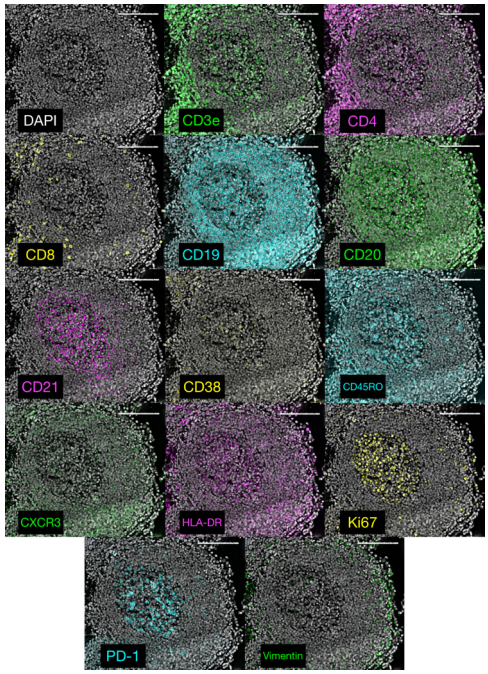

Figure 1: Representative images of expression for some antibodies for one germinal center from the cancer-reactive lymph node. DAPI is shown in white. Color denotes protein as indicated. The scale bar represents 720µm for each image.

We first asked whether proteins typically associated with T cells were indeed identifiable. To do this, the antibodies employed in downstream analysis were selected based on a combination of the signal quality and prior literature.[9,24] We observed expression of CD3e, CD4, CD8, CD45RO, and PD-1 in the GCs and T cell zones outside of the follicular mantle in accordance with prior studies.[9] We then asked whether a similar association was found with B cells. Again, there was robust signal for proteins such as CD19, CD20, CD21, Ki-67, and HLA-DR inside the GC and in the follicular mantle, also in accordance with previous investigations.[24] Other antibodies, including Vimentin, Pan-cytokeratin, PD-L1, and Mac2/Gal3, are not expressed by cells in the GC and were excluded from further analysis. In addition, proteins such as Foxp3, ICOS, PAX5, T-bet, IRF4, CD11c, CD38, and CXCR3 did not show reliable staining in all regions of both tissue samples, so they were also not included in downstream analysis. These data demonstrate that CD3e, CD4, CD8, CD19, CD20, CD21, CD45RO, HLA-DR, Ki-67, and PD-1 could be used to identify relevant adaptive immune cells.

Next, the segmentation was evaluated for accuracy (Figure 2). Here, we asked whether the segmentation algorithm could distinguish cell boundaries such that only one nucleus was assigned to each region versus manual assessment. Across three distinct tissue regions, there were 114 errors out of 1438 total segmentation events, representing a 92% segmentation accuracy.

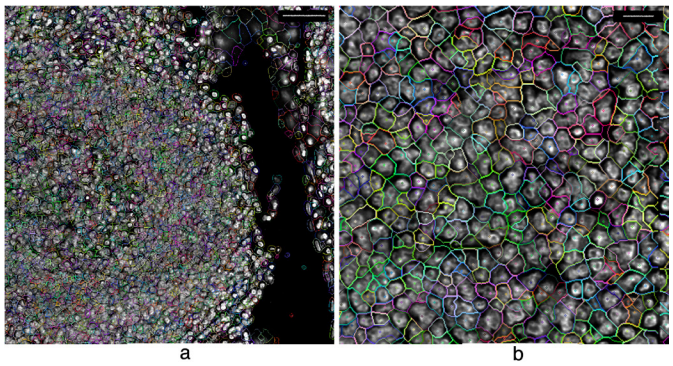

Figure 2: Segmentation overlay is shown for a cancer-reactive lymph node. DAPI is shown in white. Colored lines represent software-generated cell boundaries. The germinal center (scale bar is 360μm) (a) is also shown at higher magnification (scale bar is 80μm) (b).

To test whether known GC cell populations were identified, we manually drew boundaries around each GC in both samples based on the relative DAPI levels, CD21 expression, and Ki-67 expression in each follicle (Figure 3a). The X-shift clustering algorithm[24] was used to classify the GC cells into different subsets. This algorithm was performed first on B cells and separately for T cells. B cells clustered into two major clusters based on the expression of Ki67, whereas T cells clustered into three clusters representing T_{fh} $CD4^+$, non-Tfh $CD4^+$, or $CD8^+$ T cells.[9] These results affirmed that the adaptive immune cells in the GC could be studied using this immunofluorescent method.

Next, to validate the results of the clustering algorithm, the relative expression levels of the antibodies used in analysis on each cell population identified were mapped (Figure 3b, 3c) and compared to the literature.[22] We asked whether the expected proteins associated with B cells were indeed expressed on the GC-B cells. We found that CD19, CD20, CD21, and HLA-DR were expressed on these cells, with Ki-67 also highly expressed on the cells in the Ki-67+ cluster, as expected. Similarly, $CD4^+$ T cells and Tfh cells had higher expression of CD4 than other clusters, whereas $CD8^+$ T cells had the highest CD8 expression. T_{fh} cells were identified as the subset of $CD4^+$ T cells expressing PD-1, as PD-1 is strongly expressed on T_{fh}.[9] All three T cell subgroups expressed more CD3e and CD45RO than the B cell clusters. These data demonstrated that the clustering algorithm identified cell subsets appropriately.

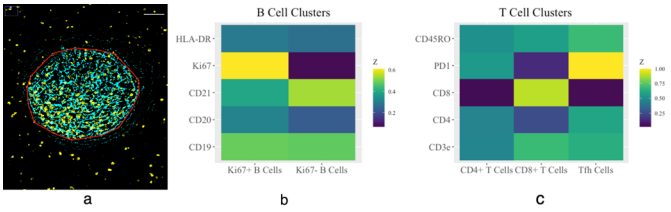

Figure 3: Clusters generated by the X-shift algorithm were evaluated for protein expression. a) Boundaries were manually drawn to identify GC areas, then these cells underwent high-dimensional clustering. Cyan represents CD21 and yellow represents Ki67. The scale bar in the top-right is 240μm. b) Heatmap showing relative expression levels of proteins on B cell subsets generated by the clustering algorithm. c) Heatmap showing relative expression levels of proteins on T cell subsets.

2. Comparing Morphological Characteristics of Germinal Centers:

We next asked whether the GCs in the cancer-draining lymph node were qualitatively different from GCs in the tonsil. GC boundaries were manually determined to facilitate the identification of cells within the GC in the healthy (Figure 4a) and cancer-reactive (Figure 4b) tissues.

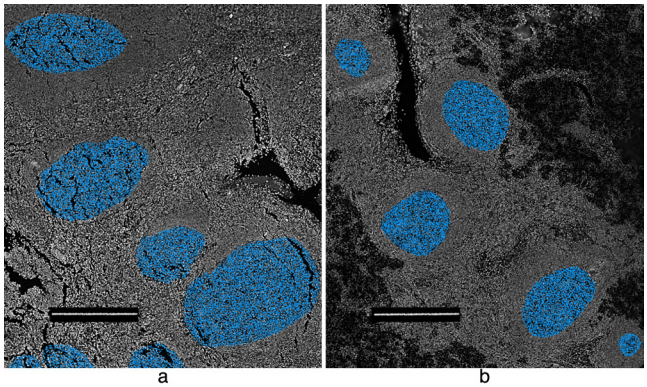

Figure 4: Germinal centers were manually identified based on tissue morphology (blue). The white scale bar is 2.25mm in both images. a) GCs in the healthy tonsil tissue. b) GCs in the cancer-reactive lymph node.

We first asked if there was a difference in the number of GCs relative to the tissue area. The total number of GCs in each sample was divided by the area of each tissue (in mm^2) to find the number of GCs per unit area (Figure 5a). There were 18 GCs in the cancer-reactive tissue sample and 7 GCs in the non-cancer-reactive tissue. We found that the density of GCs was higher in the tonsil sample (0.2 GCs/mm^2) than in the lymph node sample (0.09 GCs/mm^2). We then asked if the proportion of all cells in a GC differed between the two

DOI: 10.36838/v5i4.1

samples. A greater proportion of all cells in the tissue section were located in the GCs in the tonsil than in the cancer-reactive lymph node (Figure 5b). Indeed, 8% of lymph node cells in the cancer-reactive lymph node were in GCs while 13% of tonsil cells were inside GCs. Finally, we assessed whether GCs were similarly sized. To do this, we identified the total number of cells in each GC and compared the averages in each tissue (Figure 5c). The tonsil GCs contained more cells than the lymph node GCs, as the average lymph node GC had 929 cells, compared to 2641 cells in the tonsil GCs. To determine statistical significance, we used a two-tailed hypothesis t-test, where the two sample sizes were the number of GCs analyzed in each tissue, and the comparison was performed on the mean number of cells per GC in both tissues. We obtained a p-value of 0.007, indicating that the observed differences in GC size are significant.

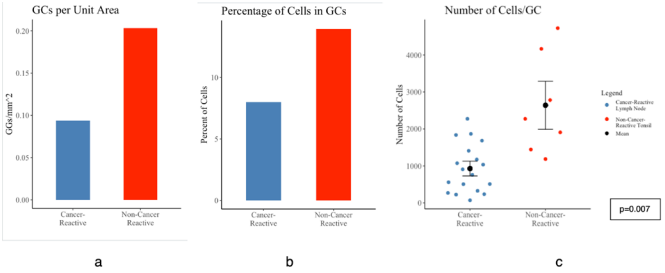

Figure 5: Comparison of germinal centers from cancer-reactive lymph and tonsil. a) The number of GCs counted per square millimeter in the cancer-reactive lymph node and tonsil. b) The percentage of cells in GCs relative to all cells in the tissue in the cancer-reactive lymph node sample and the tonsil. c) Number of cells per GC. Error bars were constructed using an 80% confidence interval.

3. Comparing Cellular Characteristics of Germinal Centers:

To assess the cellular differences between the GC in different tissues, we compared the clusters generated by X-shift clustering between the cancer-reactive lymph node and the tonsil control. B cells constituted the majority of cells in both tissues, followed by CD4$^+$ T cells, while CD8$^+$ T cells were relatively rare (Figure 6a, b).

To quantitatively assess whether there were differences in GC composition, we determined the proportion of each cellular subset in the germinal centers by dividing the total number of each cell type across all GCs by the total number of GC-resident cells (Figure 6c). We also showed a relative difference in the cancer-reactive lymph node GC cell populations from the non-cancer-reactive GC cell populations (Figure 6d). We observed 413% and 49.9% more CD8$^+$ T and T_{fh} cells, respectively, in the cancer-reactive GCs relative to the non-cancer-reactive GCs. These data suggest that while the composition of germinal centers is mostly similar across tissues, CD8$^+$ T cells and T_{fh} cells were significantly more abundant in the tumor-draining tissue. Figures 6e and 6f also show the differences in CD8$^+$ T cells and T_{fh} cells in cancer-reactive GCs and non-cancer-reactive GCs. We again used two-tailed hypothesis t-tests to determine statistical significance, where the two sample sizes were the number of GCs analyzed in each tissue type, and the comparisons were performed on the averages of the proportions of CD8$^+$ T cells and T_{fh} cells in each GC for the two tissue types. We obtained p-values of 0.008 for the comparison of CD8$^+$ T cells and 0.025 for the comparison of T_{fh} cells, again indicating that the observed differences in the proportions of these two cell types are meaningful.

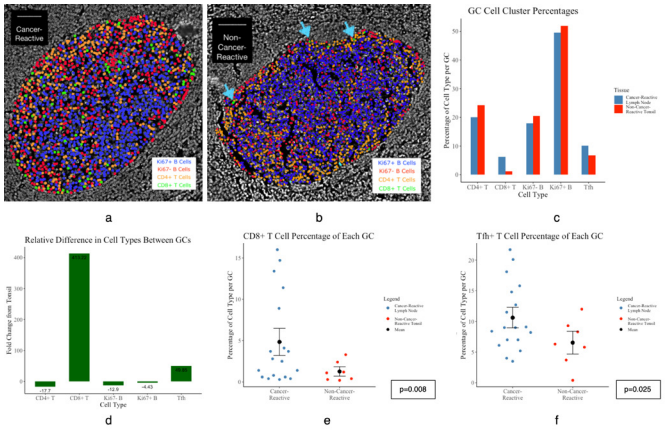

Figure 6: A cancer-reactive lymph node (a) and non-cancer-reactive tonsil (b) germinal center. Cell identities colored as shown. Blue arrows identify some CD8$^+$ T cells. The scale bar represents 360μm. (c) GC cellular subset composition in the proportion of GC cells that were B, CD4$^+$ T, CD8$^+$ T, Tfh, Ki67$^+$ B, and Ki67$^-$ B cells for both the tonsil and the lymph node. (d) The percent difference in proportions in subset composition in the cancer-reactive lymph node GCs compared to the tonsil GCs. (e) Percentage of CD8$^+$ T cells in each GC. Error bars were constructed using an 80% confidence interval. (f) Percentage of T_{fh} cells in each GC. Error bars were constructed using an 80% confidence interval.

■ Conclusion

This research aimed to identify differences between cancer-reactive and non-cancer-reactive germinal centers using multiparameter immunofluorescent imaging of tissue because patients with cancer-reactive GCs have been shown to be associated with having higher likelihoods of survival. Using the CODEX platform, we compared GCs from a tumor-draining thoracic lymph node with GCs from a non-cancerous tonsil. We made several observations during this study. Using an optimized panel of antibodies targeting key proteins in the GC, we identified major cell types using manual and high-dimensional methods in each tissue. We looked at the levels of B cells, CD4$^+$ T cells, CD8$^+$ T cells, and Tfh cells, which are the most common lymphocytes that interact inside GCs. We found fewer GCs in the cancer-reactive tissue from these data compared to the non-cancer-reactive tissue. However, the GCs in the cancer-reactive GCs had more CD8$^+$ T cells and T_{fh} cells. Together, these data highlight the importance of incorporating spatial biology into studying the immune response to cancer.

Our data observed qualitative and quantitative differences in GC biology between the two tissue types. The higher percentage of cells in GCs, number of GCs per unit area, and number of cells per GC in the non-cancer-reactive GCs (Figure 5) were likely due to the noncancerous GCs being derived from tonsils. Tonsils are exposed to high levels of antigens derived from the mouth and upper airway,[26] and tonsillar GCs have been studied as the "prototypical" GC in humans for decades. On the other hand, lymph nodes are likely less exposed to oral bacterial antigens and thus harbor less GC activity. Higher antigen exposure has been shown in previous literature to be correlated

to an increase in GC formation,[27] thus the positions of the two SLOs in the human body could make a difference in the sizes and quantities of GCs. However, other qualitative differences remain, as the cellular composition of healthy tonsil GCs and healthy lymph node GCs has been shown to be similar.[20] We observed differences in the proportions of different cell types in noncancerous and cancer-reactive GCs, with elevated numbers of $CD8^+$ T cells and Tfh cells in the cancer-reactive GCs (Figure 6a-e). Thus, the differences observed here may reflect immune responses to the nearby tumor.

In previous studies, $CD8^+$ T cells are associated with the maintenance of cytolytic potential in the tumor and the lysis of tumor cells.[28,29] Because of their well-described role in elimination of tumor cells, it is possible that they are a key factor in cancer-reactive GCs being associated with improved survival likelihoods. However, it is unclear when and where these cells are "licensed" to join the immune response. We observed a higher proportion of $CD8^+$ T cells in some, but not all, GCs in the cancer-draining lymph node relative to tonsillar GCs. One possibility is that only some of the GCs in the cancer-draining lymph node respond to the tumor, whereas the others may not be tumor-reactive. Because tumor-infiltrating $CD8^+$ T cells are associated with improved survival,[7] determining whether the GCs in the tumor-draining lymph node with high $CD8^+$ T cell counts are indeed tumor-reactive would be of great interest. Indeed, the increased presence of $CD8^+$ T cells in cancer-reactive GCs could indicate an important role for these cells in the immune response to cancer.

Further study of additional proteins in these $CD8^+$ T cells would help clarify their phenotype and provide deeper insights into the specific roles that they may play in cancer-reactive GCs. For example, expression of Tim3 could imply reduced functional exhaustion, whereas positivity for CXCR5 could confirm the $CD8^+$ T cells' ability to promote an antitumor response.[27-30] Future experiments could ask whether $CXCR5^+CD8^+$ T cells or $Tim3^+CD8^+$ T cells, among other subsets, are increased in cancer-reactive GCs. It is important to understand exhaustion and activation levels in addition to just the number of $CD8^+$ T cells to understand whether these cells are actually having an impact on the tumor response. Such investigations into how these $CD8^+$ T cells interact with and influence tumors would help assess how to expand the improved outcomes to all patients.

Previous studies[31] have also indicated that the $CD8^+/T_{fh}$ cell axis also has an important role in the cancer response. The accumulation of T_{fh} cells is an important contributor to antitumor responses that depend on cytotoxic $CD8^+$ T cells, and the absence of T_{fh} cells can lead to $CD8^+$ T cell dysfunction, lower cytokine production, and reduced cytotoxic capabilities.[32] The increase in Tfh cells may be playing a role in supporting an antitumor response by the $CD8^+$ T cells. IL-21 produced by T_{fh} cells can enhance $CD8^+$ T cell function in the tumor, but little is known about whether this occurs outside the tumor as well. Future studies will be needed to assess whether this mechanism is occurring in cancer-reactive GCs.

The data from our studies help to connect the associations between GCs and patient response to cancer with the correlation between $CD8^+$ T cells and cancer outcomes. This can highlight opportunities for future study of the relevance of cancer-reactive GCs and the potential for their targeting to improve cancer outcomes.

Acknowledgments

I would firstly like to thank Dr. Ramin Herati and his lab for their endless help with my research and data analysis. I would also like to thank my science research teacher, Ms. Jen Doran, for her consistent support, and the IJHSR team for providing the unique opportunity for me to present this work.

References

1. Dela Cruz, C., Tanoue, L., Matthay, R. *Lung Cancer: Epidemiology, Etiology, and Prevention*; Clinics in Chest Medicine 32(4), 605-64 4: December 2011.
2. Domagala-Kulawik, J. *The Role of the Immune System in Non- Small Cell Lung Carcinoma and Potential for Therapeutic Intervention;* Translational Lung Cancer Research 4(2), 177-190: April 2015.
3. Salina, K., Solterman, A., Attar, F., Casanova, R., Uckeley, Z., Thut, H., Wandres, M., Isajevs, S., Cheng, P., Curioni-Fontecedro, A., Foukas, P., Levesque, M., Moch, H., Line, A., van de Broek, M. *Germinal Centers Determine the Prognostic Relevance of Tertiary Lymphoid Structures and Are Impaired by Corticosteroids in Lung Squamous Cell Carcinoma*; Cancer Research 78(5), 1308-1320: March 2018.
4. Mishra, A., Maruizza, R. *Insights into the Structural Basis of Antibody Affinity Maturation from Next-Generation Sequencing*; Frontiers in Immunology 9(117): February 2018.
5. Chandrasekaran, S., King, M. *Microenvironment of Tumor Draining Lymph Nodes: Opportunities for Liposome-Based Targeted Therapy;* International Journal of Molecular Sciences 15(11), 20209- 20239: November 2014.
6. Helmink, B., Reddy, S., Gao, J., Zhang, S., Basar, R., Thakur, R., Yizhak, K., Sade-Feldman, M., Blando, J., Han, G., Gopalakrishnan, V., Xi, Y., Zhao, H., Amaria, R., Tawbi, H., Cogdill, A., Liu, W., LeBleu, V., Kugeratski, F., Patel, S., Davies, M., Hwu, P., Lee, J., Gershenwald, J., Lucci, A., Arora, R., Woodman, S., Keung, E., Gaudreau, P., Reuben, A., Spencer, C., Burton, E., Haydu, L., Lazar, A., Zapassodi, R., Hudgens, C., Ledesma, D., Ong, S., Bailey, M., Warren, S., Rao, D., Krijgsman, O., Rozeman, E., Peeper, D., Blank, C., Schumacher, T., Butterfield, L., Zelazowska, M., McBride, K., Kalluri, R., Allison, J., Petitprez, F., Fridman, W., Sautés-Fridman, C., Hacohen, N., Rezvani, K., Sharma, P., Tetzlaff, M., Wang, L., Wargo, J. *B Cells and Tertiary Lymphoid Structures Promote Immunotherapy Response*; Nature 577, 549-555: January 2020.
7. Cabrita, R., Lauss, M., Sanna, A., Donia, M., Larsen, M., Mitra, S., Johassen, I., Phung, B., Harbst, K., Vallon-Christersson, J., Schoiack, A., Lövgren, K., Warren, S., Jirström, K., Olsson, H., Pietras, K., Ingvar, C., Isaksson, K., Schadendorf, D., Schmidt, H., Bastholt, L., Carneiro, A., Wargo, J., Svane, I., Jönsson, G. *Tertiary Lymphoid Structures Improve Immunotherapy and Survival in Melanoma*; Nature 577, 561-565: January 2020.
8. Stebegg, M., Kumar, S., Silva-Cayetano, A., Fonseca, V., Linterman, M., Graca, L. *Regulation of the Germinal Center Response*; Frontiers in Immunology 9(2469): October 2018.
9. Crotty, S. *T Follicular Helper Cells: A Decade of Discovery and Diseases*; Immunity 50(5), 1132-1148: May 2019.
10. Choi, S., Morel., L. *Immune Metabolism Regulation of the Germinal Center Response*; Experimental and Molecular Medicine 52, 348-35 5: March 2020.
11. Vaccari, M., Franchini, G. *T Cell Subsets in the Germinal Center: Lessons from the Macaque Model*; Frontiers in Immunology 9(348): February 2018.

DOI: 10.36838/v5i4.1

12. Ramiscal, R., Vinuesa, C. *T Cell Subsets in the Germinal Center*; Immunological Reviews 252, 146-155: March 2013.
13. Waldman, A., Fritz, J., Lenardo, M. *A Guide to Cancer Immunotherapy*: From Basic T Cell Science to Clinical Practice; Nature Reviews Immunology 20, 651-668: May 2020.
14. Coppola, D., Mulé, J. *Ectopic Lymph Nodes Within Human Solid Tumors*; Anatomic Pathology and Cutaneous Oncology 26(27), 43 69-4370: September 2008.
15. Bratchel, E., Washiyama, M., Johnson, G., Tenner-Racz, K., MacLennan, I. *Differences in the Germinal Centers of Palatine Tonsils and Lymph Nodes*; Scandinavian Journal of Immunology 43, 239- 247: March 1996.
16. Im, K., Mareninov, S., Diaz, M., Yong, W. *An Introduction to Performing Immunofluorescence Staining*; Methods in Molecular Biology 1897, 299-311: December 2018.
17. McKinnon, K. *Flow Cytometry: An Overview*; Current Protocols in Immunology 120: February 2021.
18. Hwang, B., Lee, J., Bang, D. *Single Cell RNA Sequencing Technologies and Bioinformatics Pipeline*; Experimental and Molecular Medicine 50, 1-14: August 2018.
19. Black, S., Philips, D., Hickey, J., Kennedy-Darling, J., Venkataraaman, V., Samusik, N., Goltsev, Y., Schürch, C., Nolan, G. *CODEX Multiplexed Tissue Imaging with DNA-conjugated Antibodies*; Nature Protocols 16, 3802-3835: July 2021.
20. Goltsev, Y., Samusik, N., Kennedy-Darling, J., Bhate, S., Hale, M., Vazquez, G., Black, S., Nolan, G. *Deep Profiling of Mouse Splenic Architecture with CODEX Multiplexed Imaging*; Cell 174(4), 968-981: August 2018.
21. Phillips, D., Schürch, C., Khodadoust, M., Kim, Y., Nolan, G., Jiang, S. *Highly Multiplexed Phenotyping of Immunoregulatory Proteins in Tumor Microenvironment by CODEX Tissue Imaging*; Frontiers in Immunology 12: May 2021.
22. Du, Z., Len, J., Rashid, R., Maliga, Z., Wang, S., Aster, J., Izar, B., Sorger, P., Santagata, S. *Qualifying Antibodies for Image-Based Immune Profiling and Multiplexed Tissue Imaging*; Nature Protocols 14 (10) 2900-2930: October 2019.
23. Tang, J. *A Color Image Segmentation Algorithm Based on Region Growing*; 2010 2nd International Conference on Computer Engineering and Technology: June 2010.
24. Victora, G., Nussenzweig, M. *Germinal Centers*; Annual Review of Immunology 30, 459-457: April 2012.
25. Zhang, Z. *Introduction to Machine Learning: k-Nearest Neighbors;* Annals of Translational Medicine 4(11), 2018: June 2016.
26. Scadding, G. *Immunology of the Tonsil: A Review*; Journal of the Royal Society of Medicine 83, 104-107: February 1990.
27. Cirelli, K., Crotty, S. *Germinal Center Enhancement by Extended Antigen Availability*; Current Opinion in Immunology 47, 64-69: August 2017.
28. Raskov, H., Orhan, A., Christensen, J., Gögenur, I. *Cytotoxic CD8+ T Cells in Cancer and Cancer Immunotherapy*; British Journal of Cancer 124, 359-367: September 2020.
29. Valentine, K., Hoyer, K. *CXCR5+ CD8 T Cells: Protective or Pathogenic?*; Frontiers in Immunology 10: June 2019.
30. Avery, L., Filderman, J., Szymaczak-Workman, A., Kane, L. *Tim-3 Co-Stimulation Promotes Short-Lived Effector T Cells, Restricts Memory Precursors, and is Dispensable for T Cell Exhaustion*; The Proceedings of the National Academy of Sciences 115(10), 2455-2460: February 2018.
31. Cui, C., Wang, J., Fagerberg, E., Chen, P., Conolly, K., Damo, M., Cheung, J., Mao, T., Askari, A., Chen, S., Fitzgerald, B., Foster, G., Eisenbarth, S., Zhao, H., Craft, J., Joshi, N. *Neoantigen-Driven B Cells and CD4 T Follicular Helper Cell Collaboration Promotes Anti-Tumor CD8 T Cell Responses.* Cell 184(25) 6101-6118: December 2021.
32. Niogret, J., Berger, H., Rebe, C., Mary, R., Ballot, E., Truntzer, C., Thibaudin, M., Derangére, V., Hibos, C., Hampe, L., Rageot, D., Accogli, T., Joubert, P., Routy, B., Harker, J., Vegran, F., Ghiringhelli, F., Chalmin, F. *Follicular Helper-T Cells Restore CD8+-Dependent Antitumor Immunity and anti-PD-L1/PD-1 Efficacy*. Journal for ImmunoTherapy of Cancer 9(6): June 2021.

Author

Aadi Bhattacharya is a high school senior at Rye Country Day School in Rye, New York. He has grown interested in biological research in cancer immunology over the course of this research and hopes to study biomedical science/engineering in college.